

regions of the  $\text{CH}_4\text{-N}_2$  and  $\text{CH}_4\text{-CH}_4$  absorption.

Comparative planetology has appropriately focused on understanding the relation between the so-called terrestrial planets: Venus, Earth, and Mars. The large planets in the outer solar systems seem to represent a different type of object, not akin to Earth from an atmospheric science point of view. However, Titan does have an atmosphere of Earth-like composition and pressure. Preliminary studies of the data returned from the Voyager 1 flyby of Titan have allowed us to explore first the greenhouse effect of atmospheric gases other than  $\text{CO}_2$  and  $\text{H}_2\text{O}$  and now the antigreenhouse effect due to organic haze particles. Further investigation of Titan in the upcoming NASA-European Space Agency Cassini Orbiter and Huygens Probe mission should give us more understanding of Titan's atmosphere, one that is both strange and yet similar to our own.

#### REFERENCES AND NOTES

1. R. E. Samuelson, R. A. Hanel, V. G. Kunde, W. C. Maguire, *Nature* **292**, 688 (1981).
2. O. B. Toon, C. P. McKay, R. Courtin, T. P. Ackerman, *Icarus* **75**, 255 (1988).
3. R. E. Danielson, J. J. Caldwell, D. R. Larach, *ibid.* **20**, 437 (1973); K. Rages and J. B. Pollack, *ibid.* **41**, 119 (1979); *ibid.* **55**, 50 (1983); C. Sagan and W. R. Thompson, *ibid.* **59**, 133 (1984); R. A. West *et al.*, *J. Geophys. Res.* **88**, 8699 (1983).
4. E. Lellouch *et al.*, *Icarus* **79**, 328 (1989).
5. C. P. McKay, J. B. Pollack, R. Courtin, *ibid.* **80**, 23 (1989).
6. Toon *et al.* (2) have determined that the cloud opacity is less than 2 at  $200\text{ cm}^{-1}$  and that the particles of the cloud are probably larger than tens of micrometers. This implies that the visible optical depth is also about 2. McKay *et al.* (5) have shown that only large particles and optically thin clouds are consistent with both the Voyager data and the surface energy balance.
7. The existence of an ocean on Titan was suggested by J. I. Lunine, D. J. Stevenson, and Y. L. Yung [*Science* **222**, 1229 (1983)] on the basis of the  $\text{CH}_4$  photochemistry. However, recent radar data suggest that only small lakes may exist on Titan [D. O. Muhleman, A. W. Grossman, B. J. Butler, M. A. Slade, *ibid.* **248**, 975 (1990)]. In either case atmospheric  $\text{CH}_4$  is determined by equilibrium with this liquid reservoir.
8. Our model is described in McKay *et al.* (5); the parameters in the current best-fit model are as those listed in table III of McKay *et al.* under the no-cloud model except that: pressure  $P_0 = 10^{-4}$  mbar (correcting the misprint in McKay *et al.*), relative humidity  $\text{RH}_{\text{CH}_4}$  is taken to be 66% following Lellouch *et al.* (4), and the haze asymmetry scaling factor  $\langle \theta \rangle_h$  is 1.05. This model comes close to reproducing the temperature profile of Titan's atmosphere. The computed surface temperature is 93.67 K compared to the reported value of 93.9 K (4).
9. R. E. Samuelson, *Icarus* **53**, 364 (1983).
10. D. M. Hunten *et al.*, in *Saturn*, T. Gehrels and M. S. Matthews, Eds. (Univ. of Arizona Press, Tucson 1984), pp. 671-759.
11. We assume that in this idealized antigreenhouse the layer is isothermal because this simplifies the analysis. Isothermal conditions could be maintained by adiabatic motions if the layer were physically thin. However, in general the layer would not be isothermal and the emissions from the bottom of the layer would depend on the temperature at that point. This temperature would be determined by the internal greenhouse and antigreenhouse effects within the layer itself.

12. The effective temperature is the temperature at which a blackbody would emit the same total thermal infrared radiation as the surface and atmosphere of Titan. This must balance the total solar radiation absorbed by the surface and atmosphere. In our model calculations, the effective temperature of Titan is 82 K (5).
13. The factor  $(1/2)^{1/4}$  in temperature arises as follows: the idealized isothermal (11) antigreenhouse layer absorbs all the incoming solar radiation and emits half back to space and half to the surface. Thus, the flux reaching the surface is reduced by a factor of  $1/2$ . Temperature is proportional to the fourth root of the flux.
14. J. B. Pollack, O. B. Toon, T. P. Ackerman, C. P. McKay, R. P. Turco, *Science* **219**, 287 (1983); O. B. Toon *et al.*, in *Proceedings of the Conference on Large Body Impacts* (Special Paper 190, Geological Society of America, Boulder, CO, 1982), p. 187; R. P. Turco, O. B. Toon, T. P. Ackerman, J. B. Pollack, C. Sagan, *Science* **222**, 1283 (1983); J. B. Pollack,

*Icarus* **91**, 173 (1991).

15. B. N. Khare *et al.*, *Icarus* **60**, 127 (1984).
16. Below the tropopause it is likely that the haze particles are coated with condensing hydrocarbons, principally  $\text{CH}_4$ , and are thereby swept from the atmosphere. See (2); C. F. Frère, thesis, University of Paris XII (1989).
17. The troposphere does not emit as a graybody but the opacity of  $\text{N}_2\text{-N}_2$  dominates the spectrum (Fig. 1), and an optical depth of unity at the peak of the Planck function occurs near the tropopause. At  $130\text{ cm}^{-1}$ , near the emission peak for 73 K, an optical depth of unity occurs at an altitude of 25 km and a temperature of 73 K, in agreement with our simple estimation.
18. We thank R. E. Samuelson for a careful and incisive review that considerably improved the final paper. This work was supported by NASA's Planetary Atmospheres Program.

15 April 1991; accepted 25 June 1991

## Reversible Decrease of Gel-Solvent Friction

MASAYUKI TOKITA AND TOYOICHI TANAKA

**The friction between water and the polymer network of a gel is found to decrease reversibly by three orders of magnitude and appears to diminish as the gel approaches a certain temperature at constant volume and network structure.**

WHEN WATER PASSES THROUGH A polymer network, a frictional resistance arises between the water and the network. For a permanently cross-linked network, the friction, normalized by the viscosity of water, was expected to be independent of temperature. It was found, however, that the friction decreases reversibly by three orders of magnitude and appears to diminish as the gel approaches a certain temperature. This phenomenon occurs in spite of the fact that the network structure and the total volume of the gel, and thus the network density, are unchanged.

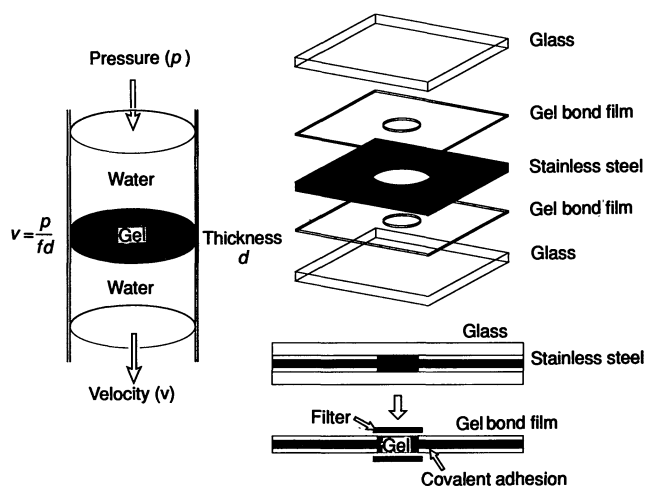
Department of Physics and Center for Materials Science and Engineering, Massachusetts Institute of Technology, Cambridge, MA 02139.

The configuration for measuring the friction coefficient of a gel is schematically shown in Fig. 1. Water is pushed through a gel slab of thickness  $d$  by a small pressure  $p$ . The proportionality between the velocity of the water  $v$  and the pressure determines the friction coefficient:

$$f = \frac{p}{dv} \quad (1)$$

To avoid any leak of water and to maintain constant gel volume, most of the gel surfaces were chemically attached to the surfaces of a pair of gel bonding plastics (Bio-Rad) by covalent bonding, except the small circular portions left open for the water flow. The open portion was mechanically pressed by rigid paper filters to prevent swelling. Small shrinkage should have oc-

**Fig. 1.** Schematic illustration of the measurements of the friction coefficient between a polymer network and water. In order to avoid any leak of water and to fix the gel volume, most of the gel surfaces (diameter 10 mm) were chemically attached to the surfaces of a pair of gel bonding films (Bio-Rad) by covalent bonding, except the small circular portions left open for the water flow. The small open portion (diameter 2 mm) was mechanically pressed by rigid paper filters to prevent swelling.



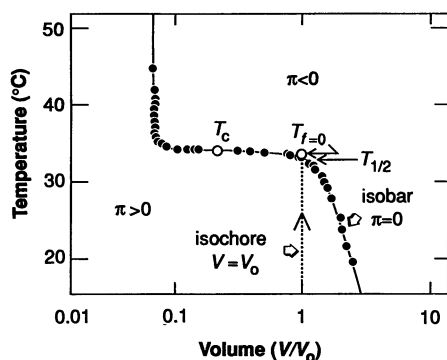


**Fig. 2.** The swelling curve (the isobar at zero osmotic pressure) of poly(*N*-isopropylacrylamide) gel in water. [Data taken from (3).] The open circles are the critical point ( $T_c$ ) and the temperature at which the friction diminishes ( $T_{f=0}$ ). The friction measurement was carried out along the isochore at the volume of gelation. At the temperature  $T_{1/2}$  the normalized friction  $f/\eta$  becomes 1/2 that at 20°C.

curred at the open portion when the temperature passed the zero osmotic pressure line, but was too small for visual observation. The details of the apparatus and the confirmation of Eq. 1 are given elsewhere (1).

The sample gel was prepared by free radical polymerization (2): 7.8 g of *N*-isopropylacrylamide (main constituent, NIPA, Kodak), 0.133 g of *N,N'*-methylenebisacrylamide (cross-linker, Bio-Rad), and 240  $\mu$ l of tetramethylethylenediamine (accelerator, Bio-Rad), and 40 mg of ammonium persulfate (initiator, Mallinckrodt) were dissolved into distilled water (100 ml) at 0°C. The gel mold was immersed into this pre-gel solution and degassed for 40 min. The temperature was raised to 20.0°C to initiate gelation.

The gel undergoes a very small discontinuous transition at 33.6°C if the gel is allowed to swell freely in water (2, 3). This corresponds to the isobar at zero osmotic pressure. The friction experiment was carried out along the isochore (constant density), but not along the critical isochore (4, 5) (Fig. 2): The gel has a lower critical point because of hydrophobic interactions (3).

When the temperature was raised along the isochore the gel presumably went into the negative osmotic pressure region, then into the coexistence regime. Temperature dependence of the swelling and shrinking behavior of the gel were checked on a sample prepared in the same mold. Without paper filters the gel slightly swelled in the open portion at lower temperatures. No visible shrinkage was observed up to the highest temperature of the friction experiment. The attachment to the gel bonding plastic remained intact in the entire temperature range.

During the friction experiment a test tube containing a gel without a mold was placed in the same water bath and the appearance of the gel was continuously monitored. At the highest temperature of our experiment, the decrease in the free gel diameter from the isochore diameter was less than 10%. These observations confirmed that the gel swelling or shrinking as a whole should not have a significant effect on the friction measurement.

A slight opacity developed in the gel near the temperature at which the friction diminished, presumably due to the dynamic density fluctuations. As we shall see later the fluctuations seem to be responsible for the diminishing of the solvent-network friction.

The temperature dependence of the friction coefficient normalized by the viscosity of water,  $f/\eta$  was measured (Fig. 3). The viscosity of water  $\eta(T)$  is taken from a table. The temperature dependence of the friction of poly(acrylamide) gel is also shown in this figure [taken from Tokita and Tanaka (1)]. The normalized friction of the poly(acrylamide) gel is independent of the temperature, while the friction of the poly(*N*-isopropylacrylamide) gel decreases three orders of magnitude as the temperature approaches 33.6°C. The change is reversible.

The phenomenon of the reversible diminishing of friction may be intuitively explained as follows. The gel-solvent friction is primarily determined by the pore size of the polymer network and the viscosity of the solvent. The latter should not show any anomaly in our experiments. When the network is homogeneous the pore size should be given by the average distance between the nearest polymer-polymer contacts. Under certain conditions, however, the polymer network undergoes substantial density fluctuations in space and time: Some portions of the gel swell while the other portions shrink maintaining, the total gel volume constant. The effective pore size is then given by the

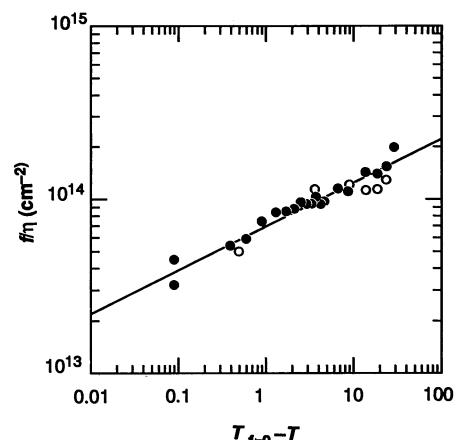
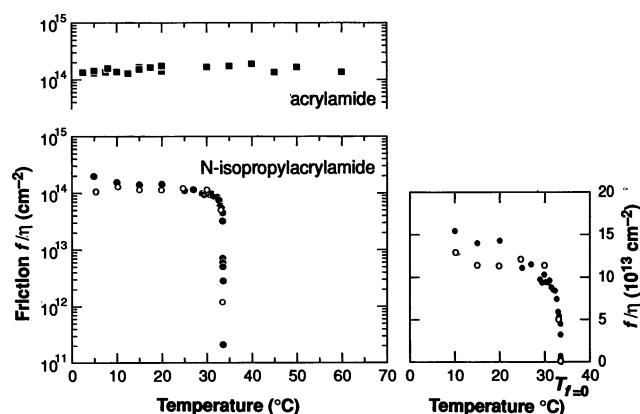


**Fig. 4.** The log-log plot of the friction coefficient, normalized by the water viscosity  $\eta(T)$ , as a function of temperature difference from  $T_{f=0}$ . The viscosity of water was taken from a standard table. The exponent is 1/4, which is much smaller than the value 5/8 predicted for dynamic spinodal fluctuations.

distance over which the network density fluctuations are correlated. The water passes through the swollen open space avoiding the shrunken regions.

The pore size practically diverges as the gel passes the coexistence curve into the two-phase region, probably for one of the following reasons: First, the gel may remain in the metastable single phase as a superheated gel. The metastable state has been observed in the hysteresis of the swelling curves of various gels including NIPA gels. The temperature gap at a hysteresis can be several degrees (3). In this case the fluctuations are dynamic (time-dependent) and should diverge on the spinodal line. Second, the gel may undergo phase separation creating domains of swollen and shrunken phases. The density fluctuations are static (time-independent) and would diverge on or near the coexistence curve. In both cases the effective pore size diverges, making the friction diminish. The pore structure is not

**Fig. 3.** The friction coefficient,  $f$ , of water passing through gels are shown as a function of temperature. Circles represent the poly(*N*-isopropylacrylamide) gel and squares represent the poly(acrylamide) gel of concentration of 8.8 g per 100 ml [taken from (1)]. Solid circles are used in the increasing of the temperature and open circles are used in the lowering of the temperature. For the NIPA gel, the friction is also plotted in the linear scale. The friction disappears at 33.6°C for the poly(NIPA) gel, whereas it is constant of temperature for the poly(acrylamide) gel.



permanent, but is reversibly enlarged or reduced with temperature.

The temperature dependence of the dynamic contribution to pore size may be estimated by means of mode coupling theory, which views a gel as consisting of  $N$  pores of diameter  $\xi$  over which the density fluctuations are correlated (6–8).

$$f = N6\pi\eta\xi \quad (2)$$

The theory further suggests

$$N = N_0 \left( \frac{\xi_0}{\xi} \right)^2 \text{ and } \xi = \xi_0 \left( \frac{T_{f=0} - T}{T} \right)^{-\nu} \quad (3)$$

where  $T_{f=0}$  denotes the spinodal temperature (that is, the temperature at which the density fluctuations diverge). Thus

$$\frac{f}{\eta} = 6\pi N_0 \xi_0 \left( \frac{T_{f=0} - T}{T} \right)^{\nu} \quad (4)$$

The least-square analysis yields  $\nu = 1/4$  and  $T_{f=0} = 33.59^\circ\text{C}$  (Fig. 4).

The determination of various critical exponents indicated that the phase transition of NIPA gels belongs to the universality class of three-dimensional Ising models (4). The exponent  $1/4$  is much smaller than the theoretical critical exponent  $5/8$  of the three-dimensional Ising model (9, 10). This discrepancy between the exponents may be because the isochore is not critical. Or it may be that the pore size diverged upon phase separation in the metastable region before the gel reached the spinodal line. In this case  $T_{f=0}$  should be considered as the temperature at which the domain size grows to infinity rather than the spinodal temperature.

By choosing an optimal combination of solvent and temperature the phenomenon should be universally observed in any gel. A drastic and reversible change in the friction may have applications in separation technology and may be relevant to some biological transport phenomena.

## REFERENCES AND NOTES

1. M. Tokita and T. Tanaka, *J. Chem. Phys.*, in press.
2. Y. Hirokawa and T. Tanaka, *ibid.* **81**, 6379 (1984).
3. S. Hirotsu, Y. Hirokawa, T. Tanaka, *ibid.* **87**, 1392 (1987).
4. Y. Li and T. Tanaka, *ibid.* **90**, 5161 (1989).
5. It will be important to study a NIPA gel prepared at the critical isochore. NIPA gel, however, became inhomogeneous upon gelation at the critical isochore because the heat generation at the critical density, that is higher than the standard density, induced a phase separation. The gel has the lower critical point due to the hydrophobic interaction.
6. T. Tanaka, S. Ishiwata, C. Ishimoto, *Phys. Rev. Lett.* **38**, 771 (1977).
7. T. Tanaka, *Sci. Am.* **244**, 124 (January 1981).
8. ———, *Phys. Rev.* **A17**, 763 (1978).
9. Y. Li, thesis, Massachusetts Institute of Technology (1989).
10. H. E. Stanley, *Introduction to Phase Transitions and Critical Phenomena* (Clarendon Press, Oxford, 1971) and references therein.
11. This work was supported by NSF and Kao Corporation. M.T. gratefully acknowledges Kao Corporation for the financial support. Authors thank W. Robertson and K. Wasserman for critical reading of the manuscript.

13 May 1991; accepted 24 July 1991

## Synchrotron X-ray Diffraction from a Microscopic Single Crystal Under Pressure

E. F. SKELTON,\* J. D. AYERS, S. B. QADRI, N. E. MOULTON, K. P. COOPER, L. W. FINGER, H. K. MAO, Z. HU

**Metallic filaments with submicrometer diameters have been fabricated. Standard diffraction techniques with conventional x-ray sources were unsuccessful in identifying the structure of these materials. However, with the use of synchrotron radiation produced on a wiggler beam line, diffraction data were obtained in measurement periods as short as 10 milliseconds. Two cylindrical single crystals of bismuth were studied, each with a diameter of  $0.22 \pm 0.02$  micrometer. The volume of sample illuminated for these measurements was 0.38 cubic micrometer, less than 0.5 femtoliter. The crystals are grown in glass capillaries, and, because bismuth expands on solidification, they are under a residual hoop stress. The crystallographic data indicate the presence of a linear compressive strain of about 2 percent, which is assumed to be the result of a residual stress of about 2 gigapascals.**

**A** MATERIALS FABRICATION TECHNIQUE has been developed that provides the ability to draw ultrafine metallic filaments. Previously, very fine wires of metals could be drawn at a temperature at which the metal is molten and confined within a softened glass capillary; the capillary is drawn into a fiber containing an axial metal filament. By cascading this process, we have been able to

produce metallic filaments with submicrometer diameters. Because of the minute quantity of material, efforts to determine the crystallographic properties of single filaments with the use of conventional x-ray sources have been unsuccessful. However, by using polychromatic synchrotron radiation produced with a wiggler insertion device (1), we have obtained structural data in measurement periods as short as 10 ms. The volume of sample illuminated for these measurements was only  $0.38 \mu\text{m}^3$ , smaller than that reported in earlier x-ray crystallographic studies. We believe that this investigation opens a new vista of opportunities for crystallographic research on a broad range of materials that can only be made in minute (submicrometer) sizes. The data were of sufficient quality to allow identification of a linear compressive strain of about 2%, which is be-

lieved to be associated with a residual stress of about 2 GPa.

The fabrication process is an extension of a method described by Taylor (2). The Taylor process, as it is sometimes called, involves melting a small amount of metal within a glass capillary and then drawing a fiber from the softened glass. By using small-diameter capillaries and pulling them quickly, so as to reduce them to a small diameter before the glass cools below its working temperature, Taylor produced fibers as fine as  $1 \mu\text{m}$  in diameter containing even finer filaments. Apparently there have been few subsequent efforts to produce submicrometer-diameter filaments by this process, although considerable research has been devoted to developing related methods for producing these materials; much of this is reviewed by Donald (3).

In the method reported here we used a Taylor wire as a starting material and two different glasses, one of which has a substantially higher working temperature than the other. First a Taylor wire of Bi was drawn with GE 180 aluminosilicate glass in an apparatus that radiatively heated the feed material with an inductively heated silicon carbide ring. The glass capillary was advanced into the hot zone at a constant rate as the fiber was drawn from the bottom. Because Bi expands on solidification, it was necessary to draw the initial fiber slowly to prevent this expansion from splitting the fiber. Pulling at a speed of about  $1 \text{ cm s}^{-1}$  resulted in unidirectional solidification along the fiber axis and permitted the volume expansion to be accommodated by a flow of excess liquid up into the melt pool maintained within

E. F. Skelton, J. D. Ayers, S. B. Qadri, N. E. Moulton, K. P. Cooper, Condensed Matter and Radiation Sciences Division and Materials Science and Technology Division, Naval Research Laboratory, Washington, DC 20375.

L. W. Finger, H. K. Mao, Z. Hu, Geophysical Laboratory and Center for High Pressure Research, National Science Foundation Science and Technology Center, Carnegie Institution of Washington, Washington, DC 20015.

\*To whom correspondence should be addressed.